doi:10.3772/j.issn.1006-6748.2021.01.010

Experimental study on integral axial squeeze film damper to suppress longitudinal vibration of propulsion shafting①

Fan Wenqiang (范文强), He Lidong②, Jia Xingyun, Yan Wei, Zhu Gang, Wang Jian
(Engineering Research Center of Chemical Safety Ministry of Education, Beijing University of Chemical Technology, Beijing 100029, P. R. China)

Abstract

This paper aims at investigating the effectiveness of squeeze oil film in suppressing the longitudinal vibration of propulsion shaft systems through a novel integral axial squeeze film damper (IASFD). After designing the IASFD, a propulsion shafting test rig for the longitudinal vibration control is built. Longitudinal vibration control experiments of the propulsion shafting are carried out under different magnitude and frequency of the excitation force. The results show that both IASFD elastic support and IASFD elastic damping support have excellent vibration attenuation characteristics, and can effectively suppress the longitudinal vibration of the shaft system in a wide frequency range. However, IASFD elastic damping support has a more significant vibration reduction effect than the other supports, and increasing the damping of the system has obvious effect on reducing the shafting vibration. For an excitation force of 45 N, the maximum reduction of the vibration amplitude is 89.16%. Also, the vibration generated by the resonance phenomenon is also significantly reduced.

Key words: integral axial squeeze film damper (IASFD), propulsion shafting, longitudinal vibration, vibration damping

0 Introduction

When the ship is sailing, due to the uneven flow field in the water, the propeller is subject to pulse power, which can be transmitted to the ship's shell through the propulsion shafting system and the foundation, causing the shell to vibrate[1]. Long-term vibration makes the crew uncomfortable and affects the use of ship's precision instruments. In the military field, acoustic radiation caused by vibration is an important factor affecting the concealment of submarines[2]. Therefore, how to reduce the transmission of longitudinal vibration of propulsion shafting to the hull has become a focus on ship research.

At present, hydraulic vibration absorber, dynamic vibration absorber, and rubber isolator are among the main methods to control the longitudinal vibration of a propulsion shafting. Hydraulic damping technology is most widely used in controlling the longitudinal vibration of shafting. This technology originated in a thrust measuring equipment[3] designed by Michell Bearing. On this basis, Ref. [4] proposed a resonance changer (RC) hydraulic damper and gave its theoretical model. Ref. [5] established the mathematical model of the transmission channel of the longitudinal excitation force of a propeller shaft system. Moreover, Ref. [5] optimized the structural parameters of RC by the transfer matrix method to reduce the transmission of the exciting force to the hull. The application of a hydraulic vibration absorber reduces the axial vibration of the propulsion shafting and does not bring strong axial resonance when the propulsion shafting works at low speeds[6]. However, the structure of the hydraulic vibration absorber is complex, and it also requires an ample installation space. The dynamic vibration absorber is an additional subsystem of the propulsion shafting, which can effectively attenuate the resonance peak in a specific frequency range, thereby reducing vibrations[7]. Ref. [8] designed a magneto-rheological elastomer dynamic vibration absorber (MRE-DVA). By controlling the magnitude of current, the shear stiffness of magnet orheological elastomer changes rapidly, thereby changing the natural frequency of the dynamic vibration absorber to suppress the vibration of the shaft in a wide

① Supported by the National Science and Technology Major Project (No. 2017-IV-0010-0047), Key Laboratory Fund for Ship Vibration and Noise (No. 614220406020717), China Postdoctoral Science Foundation Funded Project (No. 2020M670113) and the Fundamental Research Funds for the Central Universities (No. JD2003).

② To whom correspondence should be addressed. E-mail: 1963he@163.com

Received on Mar. 9, 2020

frequency range. However, excessive current amplifies the vibration of the shafting[9], and the temperature influences the properties of MRE considerably. Yang et al.[10] studied a rubber vibration isolator that can isolate the vibration transmission by embedding a rubber vibration isolator in the thrust bearing shell. The isolator has a simple structure and good impact resistance. However, at low natural frequency of the propulsion shafting, the vibration isolation effect is weak, and the isolation frequency band is narrow[11]. Subsequently, scholars successfully applied the active control technology to the longitudinal vibration of the shafting[12-13]. Ref. [13] designed an active electromagnetism dynamic vibration absorber, which generated electromagnetic force through the electromagnetic actuator to make an inertial mass oscillate with small amplitudes at the equilibrium position. The generated force offsets the longitudinal vibration of the shafting. However, active control technology strongly depends on external energy, and its parameters are difficult to control[14].

The squeeze film damper (SFD) has been widely used in aero-engines due to its excellent dynamic characteristics[15], and also in steam turbines and other rotating equipment[16]. According to some studies, the oil-film of SFD flows along the entire circumference, resulting in highly nonlinear oil film force[17-18]. Therefore, the integral squeeze film damper (ISFD) has emerged. However, the current literatures only investigate the control of the radial vibration of the rotor by ISFD[19-20], and no related research on the longitudinal vibration control of the shaft system has been found.

Therefore, based on ISFD with excellent vibration damping performance, this paper proposes and designs an integrated axial squeeze film damper (IASFD) to control the longitudinal vibration of the shaft system. The IASFD provides a certain rigidity of the shaft system and introduces additional damping to the system, thereby effectively suppressing the vibration of the shaft system in a wide frequency range. The longitudinal static stiffness of IASFD is verified through theoretical calculations and experiments. The mechanical model of IASFD for reducing the vibration is established. An experimental platform for controlling the longitudinal vibration of propulsion shafting is set up to investigate the suppression effect of IASFD on shafting vibration for different frequencies and magnitudes of the excitation force.

1 Introducing the IASFD structure

Based on the ISFD, an IASFD for controlling the longitudinal vibration of the shafting system is proposed and designed. Fig. 1 shows the structure of IASFD consisting of a cylindrical structure with internal cavities for storing hydraulic oil. In the circumferential direction of IASFD, there are squeeze film areas and an S-shaped elastomer. The squeeze film area is a discontinuous annular gap that penetrates IASFD in the radial direction and is evenly and symmetrically distributed along the circumference of IASFD. The squeezed film area can be used to store hydraulic oil and form an oil film damping effect under the action of the squeeze. The S-shaped elastomer is formed by two layers of S-shaped gaps that are nested and disconnected and is evenly and symmetrically distributed along circumference of IASFD, thus providing the devicewith specific axial stiffness. Four screws fix IASFD to the bearing block, and an O-ring is installed in the bearing block so that when IASFD is mounted in cooperation with the bearing block, a closed cavity can be formed.

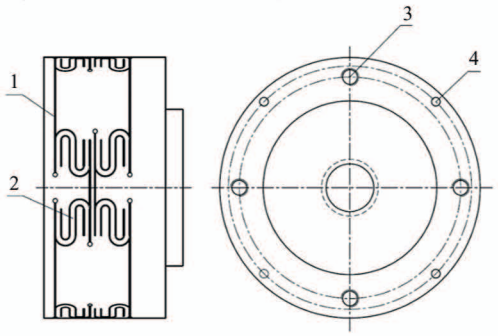

1-Squeeze film area; 2-S-shaped elastomer; 3-Threaded hole; 4-Oil inlet hole

Fig. 1 The structure of IASFD

Fig. 2 shows the 3D cross-sectional view of the shaft system consisting of IASFD, bearing block, thrust bearing, and thrust shaft. The thrust disk and the thrust ball bearing transmit the longitudinal vibration of the thrust shaft to IASFD, so the S-shaped elastomer deforms. Under the action of squeezing, the oil film in the squeeze film area of IASFD will form damping effect to suppress the longitudinal vibration of the thrust shaft.

2 Modelling the IASFD

2.1 Calculation of IASFD static load-displacement curve

The IASFD model was established in the ANSYS Work bench commercial software; the material property was set to 1Cr13. The solid 185 solid element was used, and the grid element level was fine. A fixed constraint was imposed on one end face of IASFD, and a series of increasing axial static loads from 50 N to 500 N in steps of 50 N was applied to the opposite face.

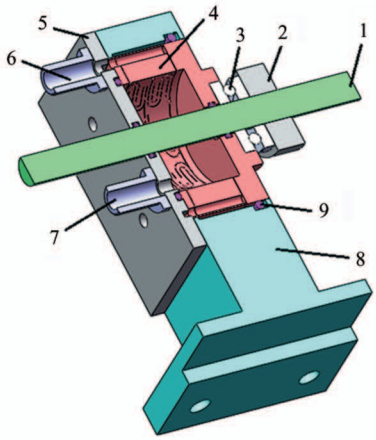

1- Thrust shaft; 2- Thrust disk; 3-Thrust ball bearing; 4-IASFD; 5-Sealed end cap; 6-Oil inlet nozzle; 7-Oil outlet nozzle; 8-Bearing block; 9-O-ring

Fig. 2 The shafting support system section of IASFD

Table 1 lists the displacement of IASFD under different static load forces. Fig. 3 shows the curve of the displacement of IASFD with the static load. Fig. 4 is the displacement cloud diagram of IASFD under static loading of 200 N.

According to Fig. 3, the axial deformation of IASFD is linear with the load so that the stiffness can be calculated by

Table 1 Displacement of IASFD under different static loads

Load/N	Displacement/mm
50	0.009822
100	0.019643
150	0.029465
200	0.039287
250	0.049108
300	0.058929
350	0.068751
400	0.078572
450	0.088394
500	0.098215

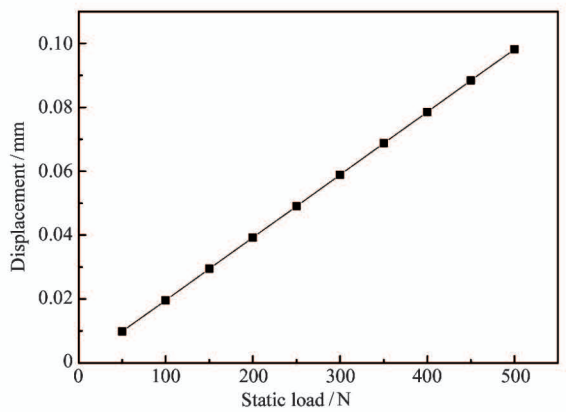

Fig. 3 Variation of IASFD displacement with static load

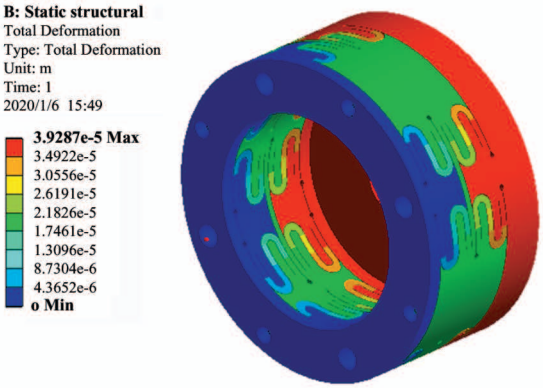

Fig. 4 Displacement cloud chart of IASFD under a static load of 200 N

$$K = \left[\sum \left(\frac{F_i}{U_i} \right) \right] / n \tag{1}$$

where, K is stiffness (N/m), F_i is load (N), U_i is displacement (mm) under the load F_i, and n is the number of loads.

Eq. (1) is used to calculate the stiffness value of IASFD under each load in Table 1; IASFD stiffness K is the average value, i. e. , $K = 5.0908 \times 10^6$ N/m.

2.2 Measurements of IASFD longitudinal static stiffness

In order to verify the above static load-displacement curve, an experimental testing bench for measuring the longitudinal static stiffness of IASFD was set up. After measuring the stiffness of IASFD, the values are compared with the calculation results from the finite element software.

Fig. 5 is a schematic diagram of IASFD longitudinal static stiffness measurement experimental bench, and Fig. 6 shows the actual test rig. The testing bench is composed of a base, an IASFD, an eddy current sensor, a magnetic base, a steel plate, and a mass. The distance from the eddy current sensor probe to the surface of the conductor is directly proportional to the output voltage of the front-end circuit. Thereby, a displacement measuring device consisting of an eddy current sensor, a front-end circuit, and a multimeter were

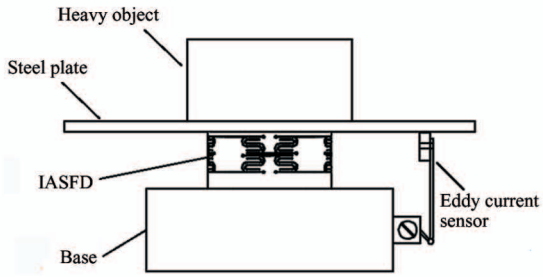

Fig. 5 A schematic diagram for measuring the longitudinal static stiffness of IASFD

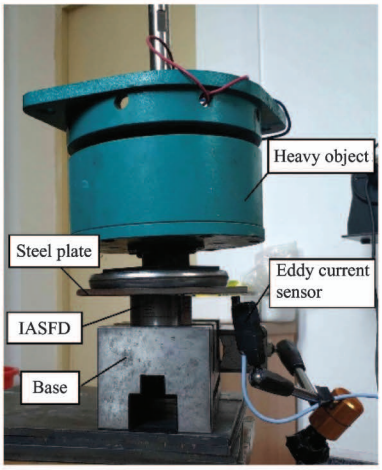

Fig. 6 The testing bench for measuring the IASFD longitudinal static stiffness

used to measure the small displacement of IASFD. The output voltage of the front-end circuit was measured with a multimeter.

The IASFD was fixed on the base first. Then, the steel plate for carrying the mass was mounted on the IASFD. Furthermore, through the steel plate, the deformation of IASFD was measured by the eddy current sensor. The multimeter reading was recorded at the beginning of the experiment (U_1) and after the mass was installed on the steel plate (U_2). Then, after removing the mass, the multimeter reading was recorded again (U_3). If U_1 and U_3 are approximately equal, it means that the installation of the mass affects the actual reading of the multimeter.

Let δ be the deformation of IASFD after installing a mass of 14.7 kg, and F the force generated by applying the mass, so $F = mg = 147$ N. Then, IASFD longitudinal static stiffness is $k = F/\delta$

In the experiment, to reduce the error, the reading satsix different locations of the sensor probe were considered. Table 2 summarizes the multimeter experimental readings.

Table 2 Experimental measurements

Measuring point	U_1/V	U_2/V	ΔU/V
1	7.75	7.47	0.28
2	9.78	9.48	0.30
3	9.67	9.48	0.19
4	6.90	6.69	0.21
5	8.41	8.16	0.25
6	8.46	8.18	0.28

In this experiment, the sensitivity of the eddy current sensor is 8 V/mm. From the experimental data, the following information is known: the average value of the voltage variation is 0.25 V; The deformation amount of IASFD after weighting is $0.25/8 = 0.03125$ mm, so the calculated stiffness of IASFD is $k = 147$ N/0.03125 mm $= 4.704 \times 10^6$ N/m.

The allowable error[21] of this experiment is 15%. Compared with the finite element calculation result of 5.0908×10^6 N/m, the error of the measured stiffness is 7.58%. Due to some uncertain factors in the experimental process, the measurement error is within the allowable error range.

2.3 IASFD discrete model

Since the IASFD can produce a specific damping force and provide a certain support stiffness for the shafting system, the device can be approximated to a spring and a damper connected in series in the shafting system. The damping of the thrust ball bearing is small enough to be negligible, so it can also be approximated as a spring. Fig. 7 shows the discrete mechanical model consisting of the bearing block, the IASFD and the thrust ball bearings.

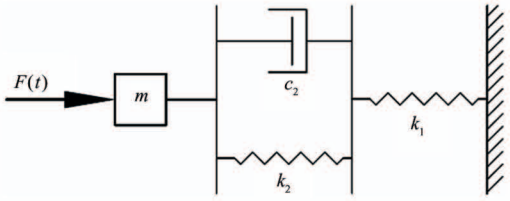

Fig. 7 The mechanical model of IASFD

where, $F(t)$ is the exciting axial force of the shafting, m is the total mass of the thrust ball bearing and IASFD, k_1 is the stiffness coefficient of the thrust ball bearing, k_2 is the stiffness coefficient of IASFD, c_2 is the damping coefficient of IASFD. The stiffness of the thrust ball bearing and IASFD are connected in series, and the stiffness after connection is $k = (k_1 \cdot k_2)/(k_1 + k_2)$. The stiffness k of the series is less than that of IASFD. The designed IASFD stiffness is much smaller than that of thrust ball bearings so that thrust ball bearings can be approximated as a rigid body. The discrete model (Fig. 7) is further simplified to the mechanical model as shown in Fig. 8, where k is the stiffness coefficient of the support system, and c is the damping coefficient of the support system.

The differential equation of motion of the simplified system is

$$m\ddot{x}(t) + c\dot{x}(t) + kx(t) = F(t) \quad (2)$$

The transfer function of the vibration system is obtained by Lagrange transformation of the above equation:

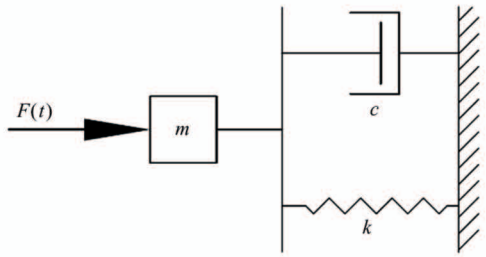

Fig. 8 Simplified model of IASFD support system

$$| G(s) | = \frac{1}{ms^2 + cs + k} \tag{3}$$

Let $s = i\omega$, then the amplitude-frequency characteristic of the system is

$$| G(i\omega) | = \frac{1}{[(k - m\omega^2)^2 + c^2\omega^2]^{1/2}} \tag{4}$$

For a vibration system with an excitation force $F(t) = F_0\cos(\omega t)$, the analytical formula for the amplitude x_0 is

$$x_0 = \frac{F_0}{[(k - m\omega^2)^2 + c^2\omega^2]^{1/2}} \tag{5}$$

If the force on the system is a constant force F_0, the static displacement of the system is

$$x_{st} = \frac{F_0}{K} \tag{6}$$

The dynamic amplification factor of the system is defined as the ratio of the amplitude generated by the unit harmonic force to the static displacement generated by the unit constant force. The system dynamic amplification factor is

$$\beta = \frac{x_0}{x_{st}} = \frac{1}{[(1 - \lambda)^2 + 4\zeta^2\lambda^2]^{1/2}} \tag{7}$$

where, $\lambda = \omega/\omega_n$ is system frequency ratio, ω_n is natural frequency corresponding to the undamped system, $\zeta = \frac{c}{2\sqrt{mk}}$ is damping ratio of the system.

Set the original damping of the system to be c, and the increased damping after using IASFD is c_1, then the damping ratio after increasing the damping c_1 is

$$\zeta' = \left(1 + \frac{c_1}{c}\right)\zeta \tag{8}$$

From Eqs(7) and (8), IASFD can significantly increase the damping coefficient of the system, that is, it increases the damping ratio of the system, thereby reducing the dynamic amplification factor. Therefore, using IASFD in the shafting system can reduce the vibration of the shafting system.

Also, Fig. 9 shows the variation of dynamic amplification coefficient β of the system with the change of frequency ratio λ and damping ratio ζ. The more significant the damping ratio, the smaller the dynamic amplification factor, that is, the smaller the vibration amplitude of the system.

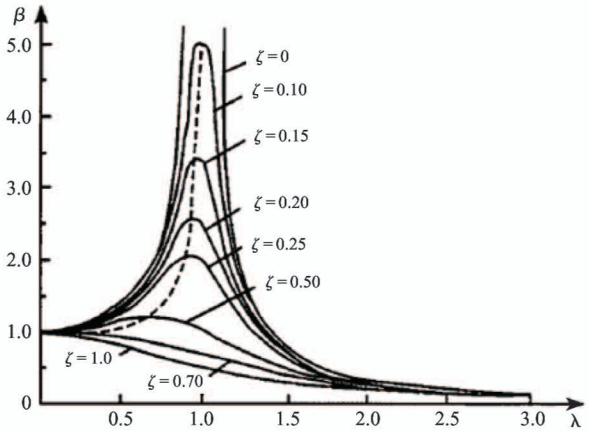

Fig. 9 The curve of amplitude changing with frequency ratio and damping ratio[22]

3 Experimental tests

3.1 Test rig description

The test bench (Fig. 10) is composed of step-less speed regulating motor, bearing block, thrust disk, IASFD, sleeve, electric vibration exciter and oil pump. The sleeve is equipped with a pair of inverted tapered roller bearings, which are used to transmit the longitudinal vibration generated by the vibration exciter to the

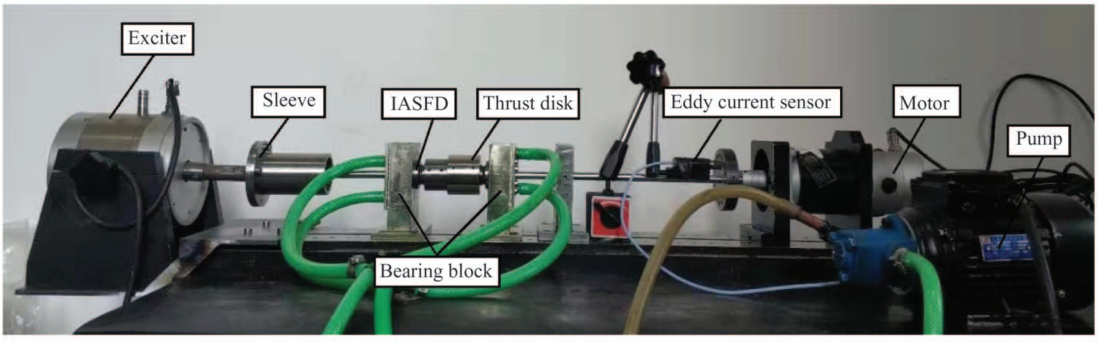

Fig. 10 Test rig for longitudinal vibration control of propulsion shafting

thrust shaft and connect the rotating thrust shaft with the main shaft of the linear vibration exciter. The motor drives the thrust shaft to rotate through the elastic coupling. The diameter of the thrust shaft, made of bearing steel, is 10 mm. The thrust shaft is fixed with a thrust disk that transmits the longitudinal vibration to the thrust ball bearings on the left and right sides and transmits the vibration to the bearing block through the thrust ball bearings. When mounted, the damping effect of IASFD absorbs the vibration in the left and right directions in the shaft system. The flexible coupling isolates the motor from the exciter, eliminating the effect of the motor on the longitudinal vibration of the shaft system.

During the experiment, an LC8000 multi-channel vibration data acquisition system was used for the vibration tests, to store and analyze the vibration data. An eddy current sensor measured the vibration amplitude of the disk on the thrust axis to obtain the longitudinal vibration of the thrust shaft.

In order to compare the vibration reduction effect of IASFD on propulsion shafting for different magnitudes and frequencies of the exciting force, the rigid sleeve and IASFD support were used in turn as a support structure for the shafting (Fig. 11). Also, comparative experiment was carried out using IASFD with and without oil supply. Without providing oil, the IASFD acts as elastic support, otherwise, it acts as elastic damping support and introduces damping into the system.

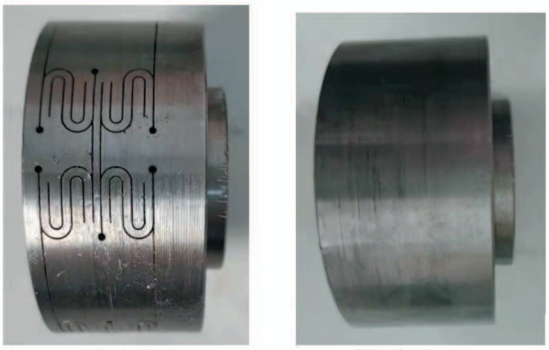

(a) IASFD (b) Rigid sleeve

Fig. 11 The two kinds of shaft support system

3.2 Results and discussion

As the main shaft speed of the propeller on the ship is 150 – 300 rpm, the motor speed was controlled at 200 rpm in the experiment.

The output force of the exciter was 15 N, and the exciting frequency varied from 5 Hz to 30 Hz in steps of 5 Hz to measure the longitudinal vibration amplitudes of the thrust shaft at different frequencies. Then the output force was increased in steps of 3.75 N until 45 N, and the above test was repeated for each step.

Fig. 12 compares the curves of vibration data measured under different working conditions.

Under different excitation conditions, compared to the rigid support, both IASFD elastic support and IASFD elastic damping support suppress the longitudinal vibration of shafting significantly. With the increase of the excitation force, the maximum amplitude of the three supports increases. The rigid support has the most

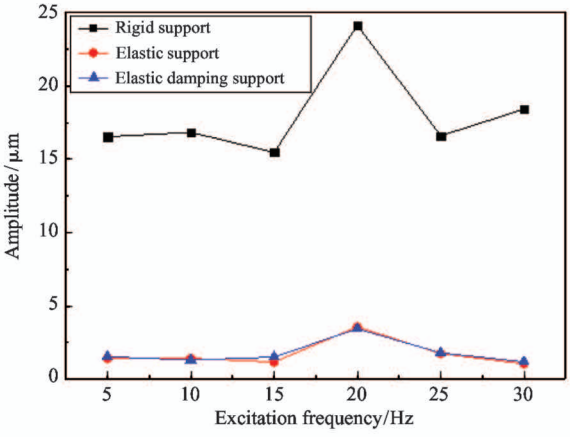

(a) 15 N

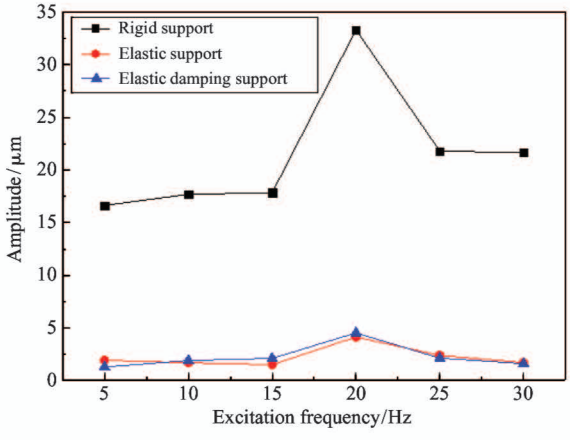

(b) 18.75 N

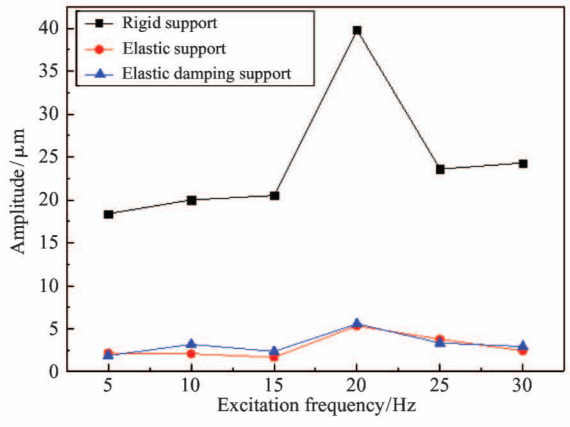

(c) 22.5 N

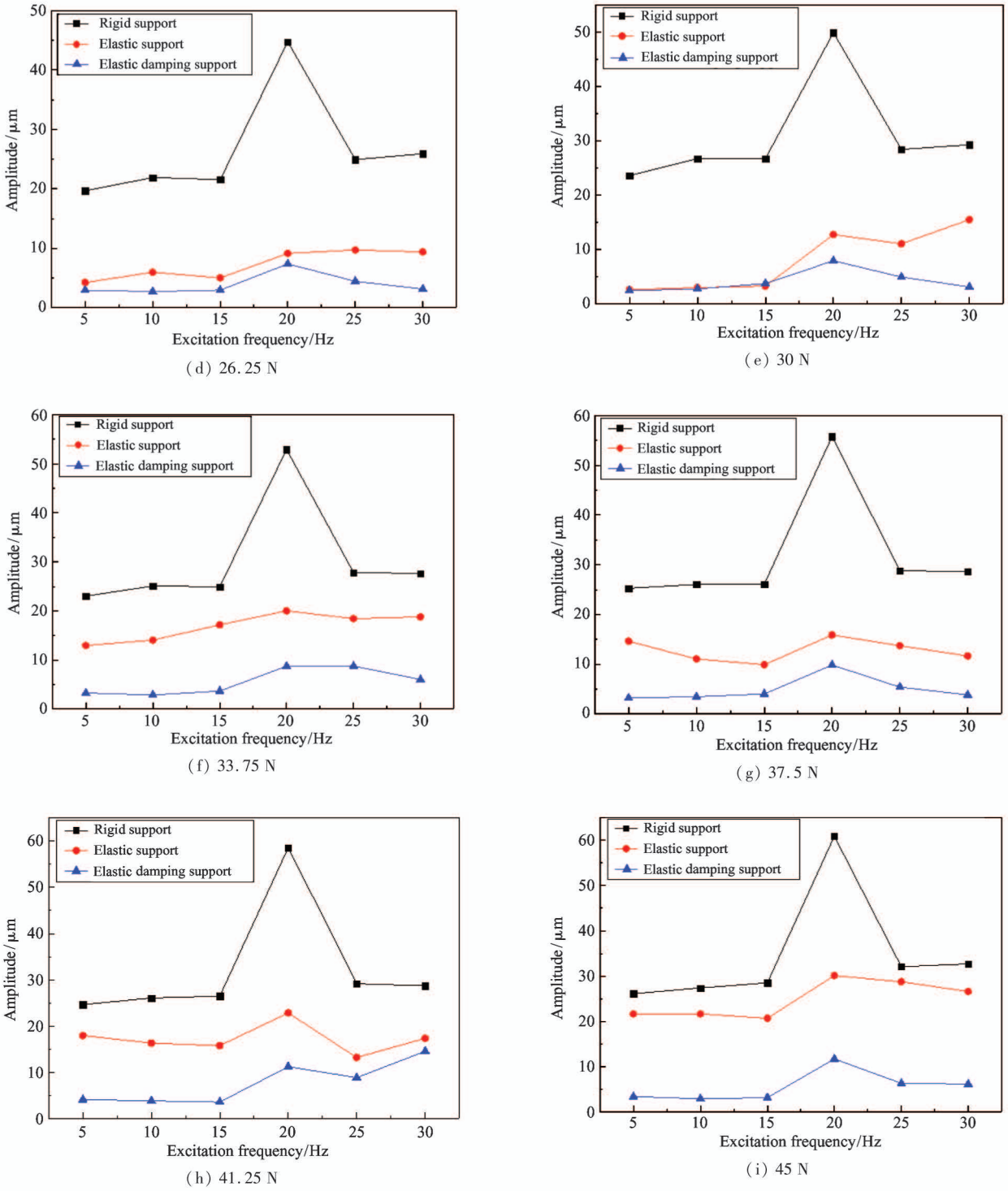

Fig. 12 Comparison of vibration amplitude of support structures under different excitation forces

significant amplitude variation, from 24.14 μm to 60.87 μm; while that for IASFD elastic damping support is relatively stable, from 1.3 μm to 26.84 μm.

For the case of rigid support, when the excitation frequency is 20 Hz, the vibration amplitude changes abruptly. In the experiment, the exciter and bracket shake noticeably at 20 Hz compared with other excitation frequencies. The analysis considers that the phenomenon maybe occurs because the excitation frequency is close to the natural frequency of the system composed of the exciter and the support, which causes the system resonance. The resonance at 20 Hz improves significantly both for IASFD elastic support and IASFD elastic damping support.

When the excitation force is between 15 N and 22.5 N, the amplitudes of the shaft under IASFD elas-

tic support and IASFD elastic damping support are almost the same because of the higher stiffness of the IASFD designed. Therefore, for small vibration amplitudes, IASFD cannot form an efficient squeezing oil film. In the range of 26.25 – 45 N, the difference between the vibration amplitudes for the two types of support gradually increases. Compared with IASFD elastic support, the vibration amplitude of the shaft with IASFD elastic damping support is smaller. One can infer that the vibration damping effect of IASFD becomes more evident with the increase of the excitation force.

In order to further compare the damping efficiency of IASFD, Table 3 and Table 4 summarize the vibration data for the excitation force of 45 N. Moreover, Fig. 13 gives the frequency spectrum of each excitation frequency of three supports for the frequency-domain comparison.

It can be seen from Table 3 that the longitudinal vibration amplitude of the shaft system is reduced to a certain extent with IASFD elastic support, compared to the case of rigid supports, with a decrease between 10.38% and 50.5%. Taking the vibration of the thrust shaft at 20 Hz as an example, when the rigid support is changed to IASFD elastic support, the vibration amplitude is reduced from 60.87 μm to 30.13 μm, decreasing by 50.5%.

Table 3 Comparison data between the rigid support and IASFD elastic support for excitation force of 45 N

Frequency/Hz	Rigid support/μm	IASFD elastic support/μm	Decrease/%
5	26.14	21.66	17.14
10	27.41	21.69	20.87
15	28.53	20.71	27.41
20	60.87	30.13	50.50
25	32.09	28.76	10.38
30	32.71	26.62	18.62

From Table 4 it can be seen that IASFD elastic damping support reduces the longitudinal vibration of the shaft system more significantly than the rigid support, with a decrease of more than 80%. Similarly, taking the vibration of thrust shaft at 20 Hz as an example, after the rigid support is replaced by IASFD elastic damping support, the vibration amplitude is reduced from 60.87 μm to 11.76 μm, and the decrease reaches 80.68%. Comparing Table 3 and Table 4, the results suggest both IASFD elastic support and IASFD elastic damping support reduce the vibration effectively, and the effect of IASFD elastic damping support is more significant than IASFD elastic support.

Table 4 Comparison data between the rigid support and IASFD elastic damping support for excitation force of 45 N

Frequency/Hz	Rigid support/μm	IASFD elastic damping support/μm	Decrease/%
5	26.14	3.45	86.80
10	27.41	2.97	89.16
15	28.53	3.21	88.75
20	60.87	11.76	80.68
25	32.09	6.37	80.15
30	32.71	6.21	81.01

Due to space limitations, considering Fig. 13(a) as an example, the frequency spectrum contains many harmonic components. At each frequency, the vibration amplitude of the rigid support is the largest, followed by the one of IASFD elastic support, while that of IASFD elastic damping support is the smallest.

IASFD elastic support and IASFD elastic damping support suppress the longitudinal vibration amplitude of the shafting effectively at each excitation frequency. Moreover, IASFD elastic damping support is more efficient in reducing vibrations than the others. In the diagrams, the vibration amplitude corresponding to the excitation frequency is the largest; compared with the rigid support, the amplitude corresponding to the excitation frequency reduces significantly after using IASFD elastic damping support.

4 Conclusion

This paper proposes the design of an integrated axial squeeze film damper (IASFD). The experimental static stiffness of IASFD was measured, and an experimental platform for the longitudinal vibration control for apropulsion shaft system was built. Under the conditions of different excitation force and frequency, the experimental research on the suppression effect of IASFD on the vibration of the shaft system was carried out. The main conclusions are as follows.

(1) In a wide frequency range, IASFD elastic support and IASFD elastic damping support both have a certain suppression effect on the longitudinal vibration of the shaft system. The vibration damping of IASFD elastic damping support with oil supply is more obvious compared to IASFD elastic support without oil supply. The results suggest the presence of the oil significantly increases the damping of the shaft system, further reducing the longitudinal vibration of the shaft system.

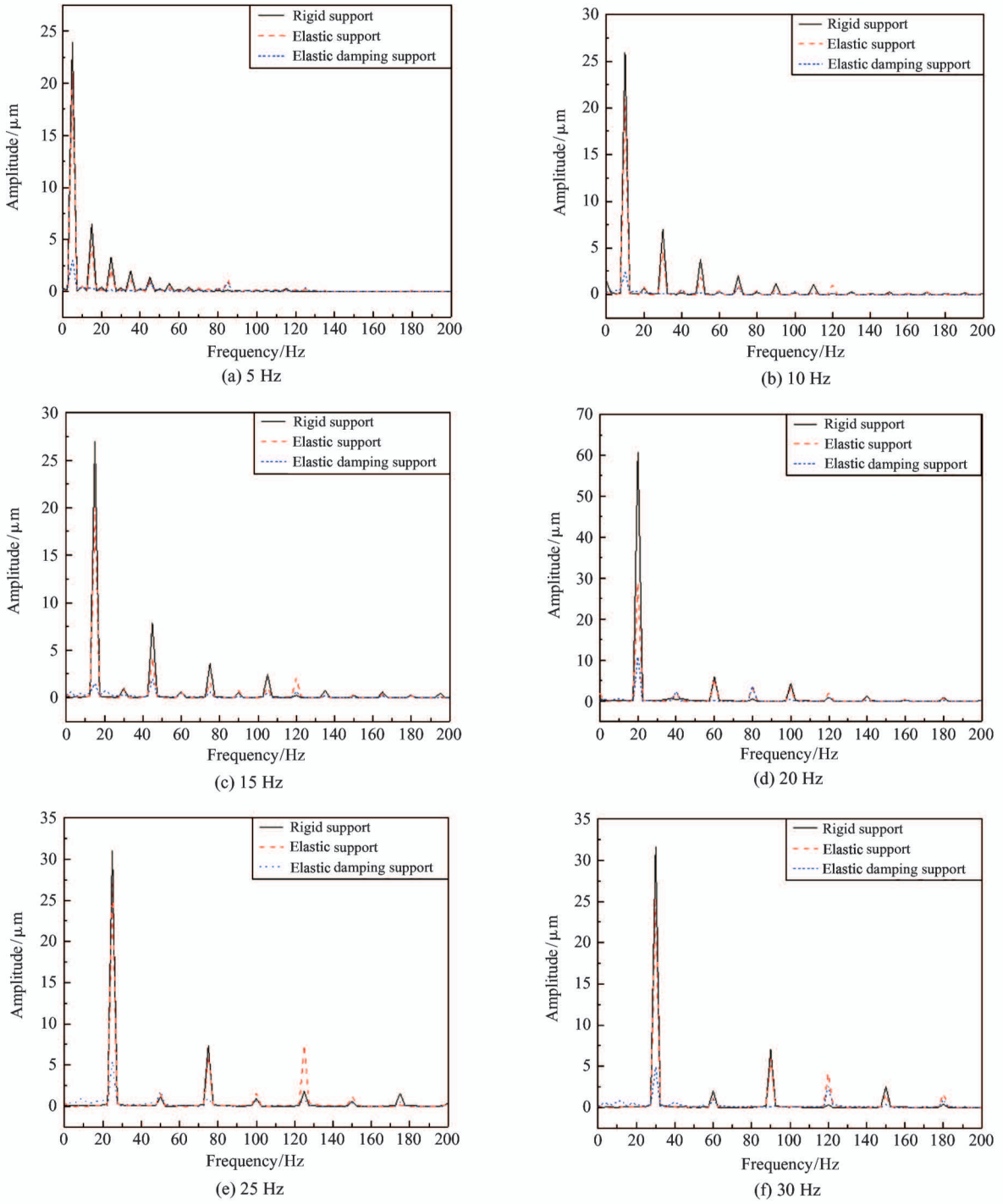

Fig. 13 Comparison of frequency spectra of support structures for different exciting frequencies when the excitation force is 45 N

(2) When the excitation frequency is close to the natural frequency of the system composed of the exciter and the bracket, an evident resonance phenomenon appears, and IASFD elastic damping support can effectively reduce the vibration due to the resonance phenomenon.

(3) With the increase of the excitation force, the maximum amplitude of the propulsion shaft system also increases. After IASFD elastic support and the elastic damping support are adopted, the vibration of the propulsion shaft system is significantly reduced. When the excitation force is 45 N, the maximum reduction of the amplitude of vibration for the elastic support is 50.5%, while for IASFD elastic damping support, it is 89.16%.

IASFD is effective in controlling the longitudinal vibration of the shafting. Further study on the influence of the oil supply pressure on the vibration reduction of IASFD elastic damping support is needed.

References

[1] Wang J S, Liu Y Z. Test and analysis of axial vibration hypostatic test rig of the ship's propelling shafting[C]// Proceedings of 2009 Mechanical Electronics Academic Conference of Electronic Mechanical Engineering Branch of China Electronic Society, Taiyuan, China, 2009: 392-396

[2] Xu J. Hiding technology of vessel[J]. *Ship Electronic Engineering*, 2010, 30(6):6-8

[3] Rigby C P. Longitudinal vibration of marine propeller shafting[J]. *Transactions of the Institute of Marine Engineers*, 1948, 60: 67-78

[4] Goodwin A J H. The design of a resonance changer to overcome excessive axial vibration of propeller shafting [J]. *Transactions of the Institute of Marine Engineers*, 1960, 72: 37-63

[5] Dylejko P G, Kessissoglou N J, Tso Y, et al. Optimization of a resonance changer to minimise the vibration transmission in marine vessels[J]. *Journal of Sound and Vibration*, 2007, 300(1-2):101-116

[6] Luo Q, Ma Y M, Ji X A, et al. Overview of resonance changer to reduce longitudinal vibration of thrust bearing in marine vessel[J]. *Ship Engineering*, 2014, 36(1):1-5, 28

[7] Liu Y Z, Wang N, Meng H, et al. Design of dynamic vibration absorbers to reduce axial vibration of propelling shafts of submarine[J]. *Journal of Vibration and Shock*, 2009,28(05):184-187, 214

[8] Li Q Y, Xie Z L, Yang Z R, et al. Experiment of dynamic vibration absorbers made of magnetorheological elastomer material[J]. *Noise and Vibration Control*, 2015, 35(4):138-142

[9] He L D, Hu H L, Feng H R. Experimental study on active vibration control of four-span rotors with magnetorheological dampers[J]. *Journal of Huazhong University of Science and Technology. (Natural Science Edition)*, 2016, 44(8):66-70

[10] Yang Z R, Qin C Y, Rao Z S, et al. Design of vibration isolator in ship's thrust bearing[J]. *Noise and Vibration Control*, 2013,33(6):211-215

[11] He J Y, He L, Shuai C G, et al. Design research of integrated vibration isolation system for marine power equipment and thrust bearing[J]. *Ship Science and Technology*, 2013, 35(1):77-81

[12] Baz A, Gilheany J, Steilmel P. Active vibration control of propeller shafts [J]. *Journal of Sound and Vibration*, 1990, 136(3): 361-372

[13] Johnson B G, Hockney R, Eisenhaure D, et al. System and method for damping narrow band axial vibrations of a rotating device[P]. US Patent: 5291975, 1994

[14] Yang T J, Jin G Y, Li W Y, et al. Study on active control techniques for warship power plant[J]. *Ship Science and Technology*, 2006, 28(S2):46-53

[15] Holmes R. The control of engine vibration using squeeze film dampers [J]. *Journal of Engineering for Power*, 1983, 105 (3): 525-530

[16] Edmund A M. Application of squeeze film dampers to a large centrifugal compressor [C] // Proceedings of the ASME Turbo Expo 2010, Glasgow, UK, 2010:409-420

[17] Shuiau T N, Wang C R, Liu D S, et al. Nonlinear dynamics study on effects of rub-impact caused by oil-rupture in a multi-shafts turbine with a squeeze film dampers [C]// Proceedings of ASME Turbo Expo 2014: Turbine Technical Conference and Exposition, Düsseldorf, Germany, 2014: 27214-27221

[18] Zhang J, Ellis J, Roberts J B. Observations on the nonlinear fluid forces in short cylindrical squeeze film dampers[J]. *Journal of Tribology*, 1993, 115(4): 692-698

[19] Ertas B, Cerny V, Kim J, et al. Stabilizing a 46MW multistage utility steam turbine using integral squeeze film bearing support dampers[C]//Proceedings of ASME Turbo Expo: Turbomachinery Technical Conference and Exposition, Düsseldorf, Germany, 2014: 1-10

[20] Ertas B, Delgado A, Moore J. Dynamic characterization of an integral squeeze film bearing support damper for a supercritical CO_2 expander[C] // Proceedings of ASME Turbo Expo: Turbomachinery Technical Confercnce and Exposition, Charlotte, USA, 2017: 1-9

[21] Shao J J, Zhang X, Miao T C, et al. Crystal plasticity model apply to the error analysis of microcompression test [J]. *Journal of Shanghai Jiao Tong University*, 2018, 52(7): 860-866

[22] Zhu S J, He L. Vibration Control of Onboard Machinery [M]. Beijing: National Defense Industry Press, 2006: 20-26 (In Chinese)

Fan Wenqiang, born in 1993. He is studying for his M. S. degree in Diagnosis and Self-recovery Engineering Research Center of Beijing University of Chemical and Technology. He received his B. S. degree in Shandong University of Science and Technology in 2017. His research interests include the longitudinal vibration control of marine propulsion shafting and vibration reduction technology of pipeline.